PHYSICAL REVIEW B VOLUME 22, NUMBER 1 1 JULY 1980

NMR study of the electronic structure of Be and *Be*Ni

M. N. Alexander,* P. L. Sagalyn, J. A. Hofmann, and W. J. Croft
Army Materials and Mechanics Research Center, Watertown, Massachusetts 02172

(Received 16 July 1979)

Measurements are reported of the ^{9}*Be*Ni Knight shift $\mathcal{K}$ in *Be*Ni alloys, and the ^{9}Be spin-lattice relaxation time T_1 in *Be*Ni and pure Be. $T_1T = (1.86 \pm 0.06)$ sec K in Be, and is constant in Be and *Be*Ni below room temperature. However, the relaxation rate is enhanced above the $1/T_1T$ level when $T \gtrsim 300$ K in both Be and *Be*Ni, the shape of $1/T_1$ vs T being the same for both metal and alloys. This phenomenon is explained in terms of the effect that thermal broadening of the Fermi distribution has on T_1 in the presence of the deep valley in the Be electron density of states, $N(E_F^0)$, at the Fermi energy. The experimental value of T_1T is combined with theoretical estimates of magnetic hyperfine interactions to give $N(E_F^0)$, and with specific-heat measurements to give the electron-phonon mass-enhancement parameter; the accuracies of these results are limited by the difference between the two theoretical values for the contact hyperfine interaction in Be. Using a simple model for T_1 based on the contact hyperfine interaction, we find that $\sim 60\%$ of the increase in $1/T_1$ upon dilute alloying with Ni can be ascribed to an increase in $N(E_F^0)$, and the remaining $\sim 40\%$ to increased hyperfine fields associated with screening of the Ni. When these results are combined with experimental susceptibility data for Be and *Be*Ni, the initial increase of $\mathcal{K}$ in *Be*Ni is correctly predicted. Finally, the anomalous electron-spin susceptibility of Be is examined in light of NMR data.

I. INTRODUCTION

The electronic properties of beryllium have for many years attracted considerable interest. Because beryllium has only four electrons, its band structure could be calculated as early as 1940.[1] That first calculation, and the many that followed,[2–13] showed there is a deep valley in the electron density of states near the Fermi energy, making Be an excellent illustration of the principle that divalent materials would be insulators if it were not for band overlap.[14]

The small density of states at the Fermi energy, $N(E_F)$, in beryllium is associated with several unusual properties. The specific heat of Be is very small,[15, 16] and so is the paramagnetic susceptibility.[17–19] The NMR Knight shift is negative and very small in magnitude,[20–22] reflecting both the small susceptibility and the small contact hyperfine field.[23] The beryllium nuclear spin-lattice relaxation time is the longest found for any metal.[20, 24–26]

Several years ago Klein and Heeger took advantage of the small $N(E_F)$ in Be to study the effects transition-metal solutes have on nontransition-metal hosts.[27] Small changes in the density of states caused by dilute alloying can be readily detected because the pure metal $N(E_F)$ is small. Klein and Heeger studied the specific heat, magnetic susceptibility, and residual resistivity of *Be*Ni, and used their results to analyze the Ni perturbation of the host in terms of the Friedel-Anderson model.[28, 29]

The work reported here also exploits the small density of states at E_F in Be to study the host NMR properties of *Be*Ni (Narath has reported parameters for ^{61}Ni in a 1 at.% *Be*Ni sample at liquid-helium temperatures[30]). The large fractional changes with alloying we find for the ^{9}Be spin-lattice relaxation time, T_1, and the Knight shift, $\mathcal{K}$, permit a reasonably accurate determination of the effects of alloying with small amounts of solute. This contrasts with the situation for nonmagnetic copper-based alloys, for example, in which changes in the ^{63}Cu T_1 with alloying are difficult to discern because the fractional change in $N(E_F)$ is small.[31]

We report room-temperature measurements of the ^{9}Be T_1 and $\mathcal{K}$ in dilute alloys of Ni in Be. The data are discussed in terms of a simple model in which the average hyperfine coupling, spin susceptibility, and density of states change with alloying, and we link our results to those of Klein and Heeger.

We also report the dependence on temperature, in the range 77–525 K, of the ^{9}Be T_1 in the pure metal and in one *Be*Ni sample. Comparison of the two sets of data permits us to account quantitatively for the anomalous enhancement of the ^{9}Be T_1 observed above room temperature,[25, 26] and to comment critically on other explanations advanced to account for the enhancement. We also use available data for pure Be to determine $N(E_F)$ for the pure metal; combining $N(E_F)$ with data from specific-heat measurements permits calculation of the electron-phonon mass enhancement parameter. Finally, we discuss, in the light of NMR results, the serious discrepancy that exists between the theoretically calculated[13] and experimentally measured[17–19] electron-spin susceptibility of Be.

II. EXPERIMENTAL

A. Samples

Our Be metal sample was a Pechiney CR-grade powder which was annealed for one hour at 800 °C and passed through a 250 mesh sieve. Analysis of a CR-grade flake showed it to be 99.5% beryllium by weight, with oxygen and chlorine the principal contaminants. Since such contaminants form insulating compounds with Be, they should not affect the electronic structure of the metal. T_1 results for a 99.9% pure sample were not significantly different from results for the 99.5% sample.

Weighed amounts of > 99.5 wt.% pure Be and pure Ni were arc melted to make the *Be*Ni alloys. The resulting materials were homogenized at about 1100 °C and quenched. The samples were inspected metallographically, and analyzed with a microprobe to ensure that no segregation had occurred. Ni concentrations obtained from the microprobe analysis and an independent wet chemical analysis both agreed with the concentration predicted from the starting materials. The samples were comminuted, passed through a 250 mesh sieve, magnetically cleaned, and vacuum annealed for one hour at 800 °C. Both the Be and *Be*Ni powders were sealed in thick-wall Pyrex tubing for the NMR experiments.

Alloul and Froidevaux found that the ^{9}Be T_1 is sensitive to residual damage due to comminution.[24] The close agreement between our T_1 results and theirs, to be described below, demonstrates the adequancy of our annealing. Moreover, since the stated purity of the Alloul-Froidevaux sample was greater than that of ours, the agreement between the T_1 results shows our samples to be sufficiently pure for this work.

TABLE I. Lattice parameters of *Be*Ni alloys.

Ni concentration c_{Ni} (atomic fraction)	c (Å)	a (Å)	c/a
0	3.5844 ± 0.0002[a]	2.2859 ± 0.0002[a]	1.5680
0.0020	3.5898 ± 0.0002	2.2876 ± 0.0002	1.5692
0.0050	3.5925	2.2875	1.5704
0.0110	3.5980	2.2878	1.5726
0.0220	3.6050	2.2893	1.5747
0.0355	3.6163	2.2922	1.5776

[a] Howard E. Swanson, Howard F. McMurdie, Marlene C. Morris, Eloise H. Evans, and Boris Paretzkin, Nat. Bur. Stand. (U.S.) Monogr. 25, Sec. 9, 64 (1971).

X-ray measurements on our powders confirmed that our *Be*Ni samples retain the α-Be structure. A high-angle diffractometer using Cu radiation and a post-sample monochromator was used. The divergence angle was 1°. The detector was a scintillation counter which was fed into a pulse-height analyzer.

There seem to be no published values of the lattice parameters of *Be*Ni alloys. Table I presents lattice parameters for our samples. In these measurements, lattice parameters were calculated with each reflection weighted according to Hess's scheme.[32] The Nelson-Riley function[33] was used to account for absorption and beam divergence. The cell size was then calculated by extrapolating 2θ to 180° and fitting by a least-squares method.[34]

The lattice parameters, c, a, and the axial ratio c/a are found to be monotonically increasing functions of Ni concentration, up to our highest concentration, 3.55 at.% Ni.

B. NMR techniques

The temperature dependence of T_1 was measured via adiabatic rapid passage techniques at 4.01 MHz. Adiabatic rapid passage through spectra split by the nuclear quadrupole interaction should produce a state which cannot be described by a spin temperature, and which therefore is characterized by nonexponential spin-lattice relaxation. In these experiments audio modulation was added to the sweep for instrumental reasons. The surprising result, which will be reported in detail elsewhere, is a modulation-induced mixing of the ^{9}Be quadrupole levels to form what appears to be a spin temperature state. The spin system then relaxes exponentially to thermal equilibrium with the spin-lattice relaxation time constant T_1.

T_1 measurements on Be and *Be*Ni at room temperature were performed with a Bruker 322*s* pulse spectrometer, operated at 11.50 MHz with a rotating field $H_1 \simeq 60$ Oe. The pulse and rapid passage measurements gave the same results, so there is no significant dependence of T_1 on NMR frequency or measurement technique in Be or *Be*Ni.

The pulse spectrometer was also used to measure Knight shifts via the off-resonance beat frequency Ω that occurs in phase-coherent detection. The differences between the Ωs of *Be*Ni samples and the Ω of a saturated aqueous solution of $\mathrm{BeCl_2}$ were measured by determining the time between the zeros of the off-resonance decays. The base line was determined by saturating the ^{9}Be signal with a burst of rf pulses [the peaks of $S(t)\cos(\Omega t+\phi)$ can be used if $S(t)$ is an exponential[35]].

Since the Knight shifts in the alloys are extremely small, each measurement was performed nine or ten times, and the results were averaged. Measurement

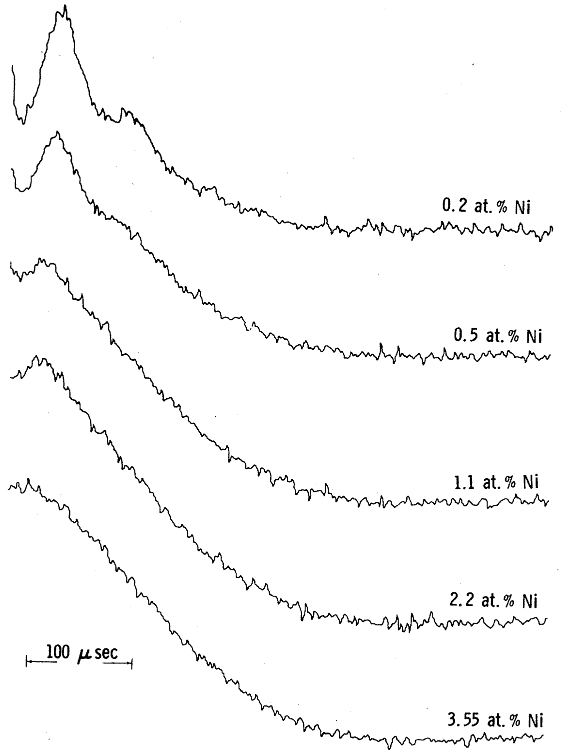

FIG. 1. Free-induction decays for ^{9}*Be*Ni powder samples at 295 K and NMR frequency of 11.500 MHz.

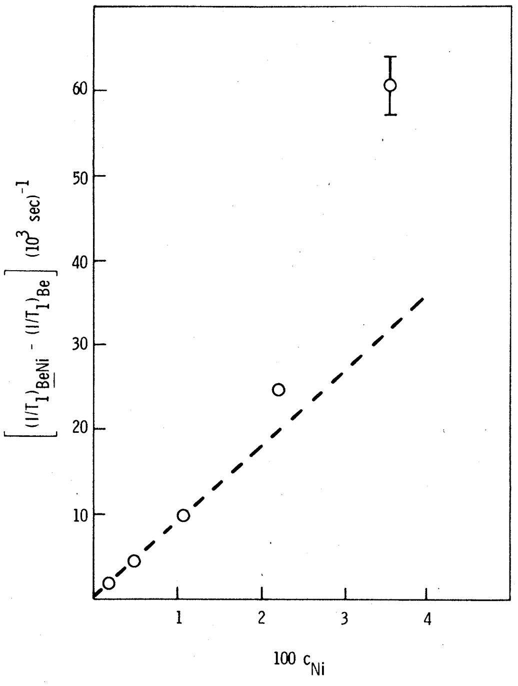

FIG. 2. Increase in ^{9}Be spin-lattice relaxation rate with alloying of Ni into Be at 295 K. The NMR frequency is 11.500 MHz.

of the time between zeros of the off-resonance decay was made more precise through operation as close to resonance as possible, thus lengthening the beat period. The upper limit on the useful beat period is set by the signal-to-noise ratio, and by the requirement that the observed zeros occur at times shorter than that at which the first zero of the Lowe-Norberg beat[36] of $S(t)$ occurs.

Another potential source of spurious zeros, in addition to Lowe-Norberg beats, is the modulation of the free-induction decay by the quadrupolar splitting.[37] This makes the off-resonance beat-frequency technique impractical for measuring the Knight shift in either the pure Be or the 0.2-at.% *Be*Ni sample, because it is difficult to disentangle the quadrupolar beats from the off-resonance beats which occur in phase-coherent detection. However, in the more concentrated *Be*Ni samples the alloying produces a distribution of quadrupole interactions which smears out the modulation of the free-induction decay—see Fig. 1—and the Knight shift can be determined via the pulse NMR technique.

III. RESULTS AND DISCUSSION

A. T_1: Dependence on c_{Ni}

The dependence on nickel concentration, c_{Ni}, of the ^{9}Be spin-lattice relaxation rate, $1/T_1$, is shown in Fig. 2 and in Table II. The enhancement of the host relaxation is proportional to c_{Ni} up to $c_{Ni} \simeq 0.011$, and differs little from proportionality at $c_{Ni} = 0.022$ (throughout this paper, c_{Ni} will be given in units of atomic fraction). Since Ni does not form a magnetic moment in Be,[27,30] deviations from the relationship $\delta(1/T_1) \propto c_{Ni}$ are probably not due to magnetic solute-solute couplings.[38]

TABLE II. Knight shift $\mathcal{K}$ and spin-lattice relaxation time T_1 for ^{9}Be in *Be*Ni. All measurements at 295 K. $\mathcal{K}$ measured relative to saturated BeCl$_2$ solution.

c_{Ni} (atomic fraction)	$\mathcal{K}$ (ppm)	T_1 (sec)
0	···	58 ± 2
0.002	···	52 ± 2
0.005	−7 ± 2	46 ± 2
0.011	12 ± 2	37 ± 2
0.022	8 ± 3	23.9 ± 0.8
0.0355	34 ± 4	12.9 ± 0.5

B. T_1: Dependence on T

Our data for the temperature dependence of $1/T_1$ for pure Be and ^9BeNi ($c_{\mathrm{Ni}} = 0.022$) between 77 and 525 K are shown in Fig. 3. Below room temperature, the usual $1/T_1 \propto T$ behavior, characteristic of nuclear relaxation via degenerate conduction electrons, holds. At 300 K and above, however, the relaxation is substantially enhanced, and the same temperature dependence holds for both Be and *Be*Ni.

Chabre, who studied Be at higher temperatures (his two lowest-temperature points, other than at room temperature, are shown in Fig. 3), also observed enhanced spin-lattice relaxation, but the enhancement he studied depended on the thermal history of his samples.[26] Samples which had been held for a long time at $T \gtrsim 1000$ K, and whose T_1's were measured immediately thereafter with *decreasing* T, exhibited a local maximum in $1/T_1$ at about 570 K. On the other hand, samples which had been kept at room temperature for a long time, and whose T_1's were then measured with *increasing* T, exhibited only a smoothly increasing enhancement of $1/T_1$. Chabre showed that the local maximum in $1/T_1$ near 570 K is caused by vacancies created at high temperature which, after becoming bound to impurities at lower temperatures, cause quadrupolar relaxation of the ^{9}Be nuclei (self-diffusion occurs at higher temperatures, where dipole-dipole relaxation dominates over quadrupolar relaxation). He did not account for the enhanced relaxation that occurred in his experimental runs with increasing temperature, however. We now show that the data in Fig. 3 indicate there must be an enhancement mechanism which depends in a fundamental way on the electronic structure of Be.

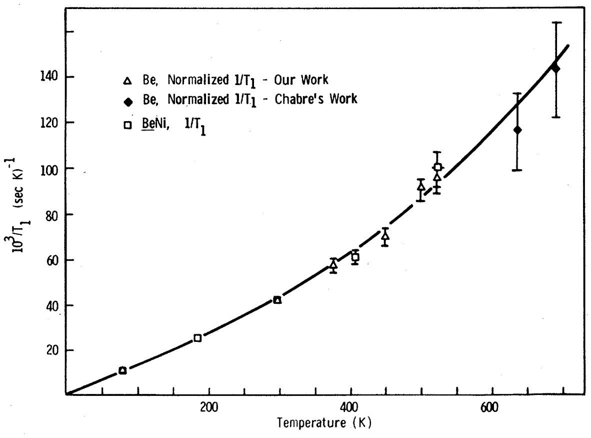

FIG. 3. Temperature dependence of ^{9}Be spin-lattice relaxation for pure Be and for the *Be*Ni sample which contains 2.2 at.% Ni ($c_{\mathrm{Ni}} = 0.022$). Equation (6) of the text was fitted to the data obtained in this study and extrapolated upward in temperature to the data points of Chabre (Ref. 26), giving the curve shown in the figure.

Suppose the enhancement of T_1 above room temperature were due to some "new" mechanism—one other than the well-known magnetic relaxation via conduction electrons, whose contribution we denote by T_{1e}. The experimentally observed T_1 should then be given by

$$(1/T_1) = (1/T_{1,\mathrm{new}}) + (1/T_{1e}) \quad . \tag{1}$$

From the data of Fig. 3 we have

$$(1/T_1)_{Be\mathrm{Ni}} = 2.44(1/T_1)_{\mathrm{Be}} \quad ,$$

and also

$$(1/T_{1e})_{Be\mathrm{Ni}} = 2.44(1/T_{1e})_{\mathrm{Be}} \quad ,$$

where the subscript *Be*Ni here refers to the $c_{\mathrm{Ni}} = 0.022$ alloy. From Eq. (1), therefore, $(1/T_{1,\mathrm{new}})_{Be\mathrm{Ni}} = 2.44\ (1/T_{1,\mathrm{new}})_{\mathrm{Be}}$. That is, the postulated "new" relaxation mechanism is stronger in the alloy than in the pure metal by precisely the same factor which relates metal and alloy in the case of the conduction-electron mechanism. That coincidence makes one suspect that the "new" mechanism must be organically related to the conduction-electron mechanism.

We now account for the enhancement of $1/T_1$ by considering the temperature dependence of the Fermi distribution of the conduction electrons. This enhancement is probably unique to beryllium because the Fermi level in Be occurs where the density of states is small and rapidly changing.

We write the nuclear spin-lattice relaxation rate in the usual form[39]

$$1/T_1 = [(64\pi^3/9)\hbar^3\gamma_e^2\gamma_n^2]\langle |u(0)|^2 \rangle_{E_F}^2 \mathcal{I} \quad , \tag{2}$$

where γ_e is the electron gyromagnetic ratio, γ_n is the nuclear gyromagnetic ratio, $\langle |u(0)|^2 \rangle_{E_F}$ is the average over the Fermi surface of the conduction-electron density at the nucleus, and

$$\mathcal{I} = -\tfrac{1}{4}kT \int_0^\infty [N(E)]^2 \left| \frac{\partial f}{\partial E} \right| dE \quad . \tag{3}$$

k is the Boltzmann constant, T is the absolute temperature, $f(E)$ is the Fermi distribution function, and $N(E)$ is the density of states per electron (the density of states in Ref. 39 differs by a factor of 2 from our density of states because the density of states for a single spin direction is used in Ref. 39). The familiar result $T_1T =$ constant results from using $(\partial f/\partial E) = -\delta(E - E_F)$ in Eq. (3), an approximation valid at most laboratory temperatures if $N(E)$ changes slowly around E_F.

The band calculations for Be, however, show there is a deep valley in $N(E)$ near E_F. Since the width of the valley is ≈ 1 eV it is possible that in the temperature range 300–800 K, corresponding to 3–8% of the valley width, the effects on T_1 of the temperature dependence of the Fermi distribution might be manifest.

To pursue this possibility we integrate Eq. (3) by parts

$$\mathcal{J} = \tfrac{1}{2} kT \int_0^\infty f(E) N(E) \left\{ \frac{\partial N}{\partial E} \right\} dE \ , \tag{4}$$

and use standard formulas for integrals containing $f(E)$ and for the temperature dependence of E_F,[40] to obtain

$$\mathcal{J} \approx \tfrac{1}{4} [N(E_F^0)]^2 kT \times \left\{ 1 + (\tfrac{1}{3}\pi^2)(kT)^2 (1/N(E_F^0)) \left[\frac{\partial^2 N}{\partial E^2} \right]_{E_F^0} \right\} \ . \tag{5}$$

In Eq. (5) E_F^0 is the Fermi energy at $T = 0$, and $[\cdots]_{E_F^0}$ means the contents of the bracket are evaluated at $E = E_F^0$; terms having order greater than T^2 have been omitted.

Thus from Eqs. (2) and (5) we have the result

$$1/T_1 \approx aT + bT^3 \ . \tag{6}$$

A least-squares fit of Eq. (6) to our data produces the curve shown in Fig. 3, with best-fit parameters $a = (1.31 \pm 0.04) \times 10^{-4}$ and $b = (1.71 \pm 0.24) \times 10^{-10}$. The value of a is equivalent to $T_1 T = (1.87 \pm 0.05) \times 10^4$ sec K for Be metal, which agrees with earlier work.[20,24] Extrapolation of our curve to higher T gives excellent agreement with the two lowest-temperature data points of Chabre (obtained with increasing T), as can be seen in Fig. 3.

The excellent fit of Eq. (6) to the data is consistent with the view that the enhancement of $1/T_1$ above 300 K is due to the thermal broadening of the Fermi distribution in the presence of the valley in $N(E)$ near E_F in Be. Of course a fit of this kind is not inherently conclusive, since other explanations might be possible. One which has the right qualitative features of our data was advanced by Jena and Das[41] in a somewhat different context—that hyperfine parameters of Be are a function of temperature. If the hyperfine parameters were a function of temperature, $(T_1)_{\mathrm{Be}}$ would remain proportional to $(T_1)_{Be\mathrm{Ni}}$, as in Fig. 3. However, the sizes of the changes with temperature of $T_1 T$ and $\mathcal{K}$ predicted by Jena and Das for Be accord poorly with experiment.

C. Knight shift

One should expect that if $T_1 T$ is a function of temperature, as we predict, the Knight shift will have a concomitant dependence on temperature. Since contributions to $\mathcal{K}$ related to the T_1 mechanism described above are proportional to the electron-spin susceptibility χ_s, we look for changes in χ_s which are related to $N(E)$. The result has been calculated elsewhere,[42] and is

$$\chi_s(T) \approx \chi_s(0) \left(1 + (\tfrac{1}{6}\pi^2)(kT)^2 \left\{ \left(\frac{1}{N(E_F^0)} \right) \left[\frac{\partial^2 N}{\partial E^2} \right]_{E_F^0} - \left(\frac{1}{N(E_F^0)} \right)^2 \left[\frac{\partial N}{\partial E} \right]_{E_F^0}^2 \right\} \right) \ . \tag{7}$$

The first term in curly brackets can be evaluated from the fitting of the T_1 data [Eq. (5) *et seq.*]:

$$(\tfrac{1}{6}\pi^2)(kT)^2 \left(\frac{1}{N(E_F^0)} \right) \left[\frac{\partial^2 N}{\partial E^2} \right]_{E_F^0} = 0.059 \ , \tag{8}$$

for $T = 300$ K.

The second term in the curly brackets of Eq. (7) is more difficult to evaluate. The only absolute thermopower measurement known to us[43] is not adequate for determining $[N^{-1}(\partial N/\partial E)]_{E_F^0}$. The numerical values of $[N^{-1}(\partial N/\partial E)]_{E_F^0}$ obtained from figures in the literature which display $N(E)$ vs E results of band-structure calculations[2,4,5,8-13] differ greatly, but nonetheless are in all cases much smaller than the first term in the curly brackets of Eq. (7).

Thus, the temperature dependence of the susceptiblity due to thermal broadening of the Fermi distribution and the valley in $N(E)$ in beryllium is

$$\chi_s(T = 300) \approx 1.06 \chi_s(T = 0) \ , \tag{9}$$

where T is the absolute temperature. If $\mathcal{K} \propto \chi_s$ the 6% change of $\mathcal{K}$ that follows from Eq. (9) could not be measured, since $\mathcal{K}$ in Be is very small.

As will be evident from later sections in this paper, however, it is not clear that $\mathcal{K} \propto \chi_s$ in Be. The negative core-polarization contribution to $\mathcal{K}$ in Be almost exactly cancels the positive contact contribution. The measured Knight shift therefore is predominantly of diamagnetic origin. There are good reasons for doubting that in Be the diamagnetic susceptibility is proportional to χ_s, as in the Landau-Peierls diamagnetism.

The experimental situation also is not clear. Barnaal *et al.* reported that $\mathcal{K} = -35$ ppm at 77 K and $\mathcal{K} = -25$ ppm at 300 K.[20] This is both larger in magnitude than, and in the opposite direction to, the prediction of Eq. (9). Chabre reported there is no change in $\mathcal{K}$ between 300 and 1200 K.[26] His experimental accuracy was ±5 ppm, or approximately 20% of $\mathcal{K}$. An analysis such as that which led to Eq. (9) predicts a $\approx 20\%$ change in $\mathcal{K}$ between 300 and 600

K, a change Chabre could not have resolved. Since the first-order expansion used to obtain Eq. (7) is inaccurate above 600 K, more cannot be said. It is clear from this discussion that the current understanding of the Knight shift in pure Be is rudimentary.

The effect of alloying of $\mathcal{K}$ is shown in Fig. 4 and Table II. The low-$c_{\rm Ni}$ portion of the plot extrapolates well to the two values of $\mathcal{K}$ for pure Be ($c_{\rm Ni}=0$) which were determined by conventional cw methods.[20,21] The third value, to which the plot does not extrapolate very well, was obtained by multiple-pulse narrowing of the dipole and quadrupole interactions.[22] One of the authors later reported an anomaly in the relative positions of the reference $BeCl_2$ and Be metal resonance lines as a function of distance from resonance.[44] We do not know how to determine the effect of this anomaly on the accuracy of the measured Knight shift.

We cannot account for the small dip in the Knight shift for the $c_{\rm Ni}=0.022$ sample. If one draws a monotonic curve through the data points for the other samples, one obtains $\mathcal{K}\simeq 24$ ppm instead of the experimental average value, $\mathcal{K}=8.35$ ppm. Use of the Student t test[45] on the hypothesis that our data are consistent with $\mathcal{K}=24$ ppm shows the probability that our experimental results would occur by chance is less than 0.005. That is, our data for the $c_{\rm Ni}=0.022$ sample are not consistent with the monotonic increase in $\mathcal{K}$ exhibited by the other alloy samples.

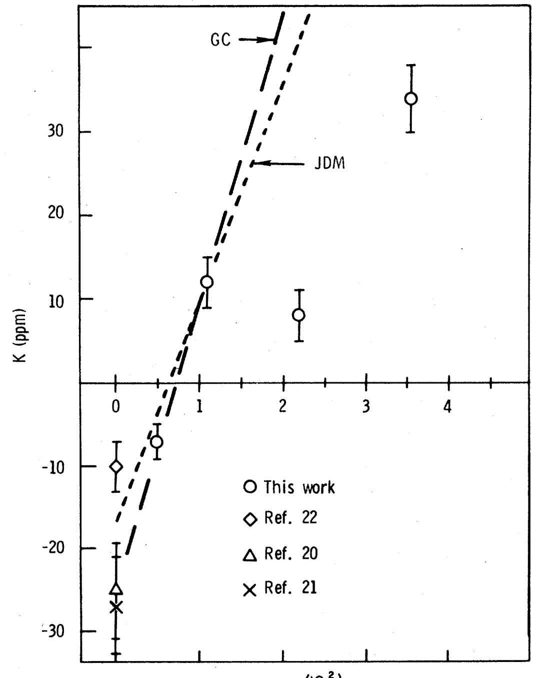

FIG. 4. ^{9}Be Knight shifts in beryllium metal and in *Be*Ni. The straight lines are predictions for the low-$c_{\rm Ni}$ behavior of the Knight shift (see Sec. IV B).

Each of our determinations of $\mathcal{K}$ involved ten separate measurements (nine in the case of the $c_{\rm Ni}=0.011$ sample). On any given day the Knight shift was measured either once or twice for every sample, the *Be*Ni samples being chosen in random order, and measurements alternating between *Be*Ni and $BeCl_2$ reference materials.

The data we cited previously—chemical analyses, lattice parameter determinations, and measurements of T_1 —give no indication that the $c_{\rm Ni}=0.022$ sample is anomalous. We did, however, find the particles in the $c_{\rm Ni}=0.022$ sample to be larger and smoother than particles in the other samples, though all samples had passed through the same mesh sieve. Klein and Heeger found no anomaly in the bulk susceptibility of *Be*Ni for $c_{\rm Ni}$ up to $\simeq 0.02$.[27] Since lack of monotonicity of $\mathcal{K}$ with solute concentation has been documented for other alloy systems,[46] our Knight shift anomaly could be real. In that event the dip in $\mathcal{K}$ vs $c_{\rm Ni}$ must arise from a contribution to $\delta(\mathcal{K})$ that does not materially affect $\delta(\chi)$.

The particles in the $c_{\rm Ni}=0.022$ sample have diameters smaller than the rf skin depth. Nevertheless, skin depth effects seem to account for the difference between the current value of $\mathcal{K}$ and the cw result reported for the same sample several years ago.[47] Probably the Be system is the only one in which this could happen, since its Knight shifts are so small. The pulse measurement should be immune to the error in the earlier cw measurement because the relative rf phases of the transmitter and receiver can be adjusted to eliminate the dispersion signal.[48] Moreover, since the Knight shifts were determined from a frequency measurement, i.e., from the off-resonance beat frequencies observed in phase-coherent detection, changes in the shape of the decay envelope (which would have been very small) due to rf skin depth effects should not affect the result.

D. Free-induction decay: Quadrupole interaction

In the hexagonal lattice of the metal the ^{9}Be nuclear quadrupole interaction results in a three-line spectrum in which a central line is flanked symmetrically by satellites. The corresponding free-induction decay has a dipole-dipole decay modulated by an oscillation characteristic of the quadrupole interaction.[37] Alloying produces a distribution of quadrupole interactions; the resulting distribution of modulating frequencies smears out the oscillation of the free-induction decay, as shown in Fig. 1.

The distribution of quadrupole couplings can be studied by quadrupole echoes since (under conditions met in our experiment) the echo envelope is the Fourier transform of the distribution function,

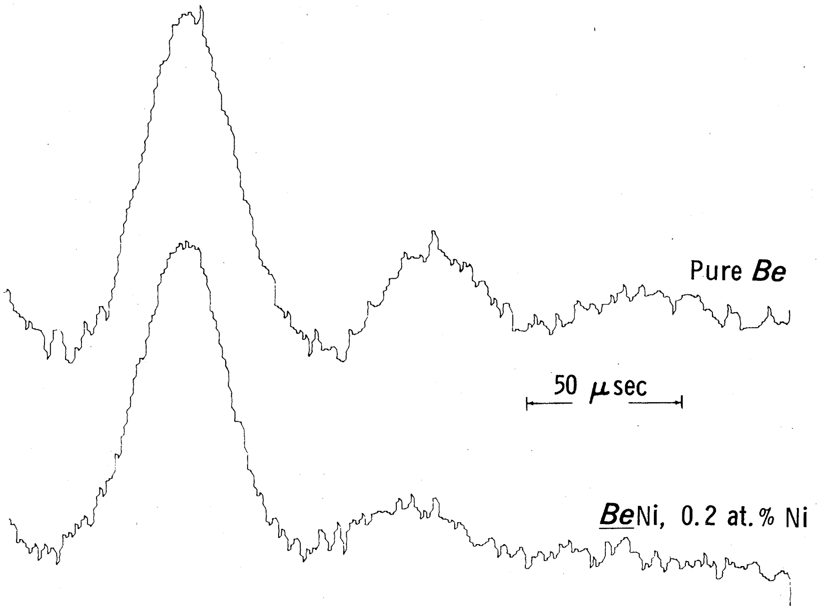

FIG. 5. ^{9}Be quadrupolar echoes in sample of pure Be powder, and in *Be*Ni powder sample which contains 0.2 at.% Ni ($c_{\text{Ni}}=0.002$), at 295 K and 11.500 MHz. The entire echo is not shown; the echo center occurs at the center of the largest peak in each echo. The lack of symmetry about a horizontal base line is due to a superimposed dipolar echo (see text).

$f(\omega_q)$, for the couplings[49] ($\omega_q \equiv e^2qQ/2h$, where Q is the nuclear quadrupole moment, q is the main electric-field-gradient component, and e is the charge of the electron). Polycrystallinity also affects the shape of the echo, since the quadrupole splitting is proportional to $\omega_q(3\cos^2\theta-1)$, where θ is the angle between the main principal axis of the electric-field gradient and the direction of the applied magnetic field.[50] A straightforward extension of the work of Ref. 24 gives for the quadrupole echo shape

$$E(t)\propto\int_0^1 d(\cos\theta)\int_{-\infty}^{\infty} f(\omega_q)\cos \times[\omega_q t(3\cos^2\theta-1)]\,d\omega_q \ , \quad (10)$$

where the center of the echo occurs at time $t=0$.

In pure Be there is a single value of ω_q, and so $f(\omega_q)$ is a delta function. $E(t)$ for a powder of pure Be is a damped oscillation, as seen at the top of Fig. 5. From Eq. (10) it can be seen how the damping is caused by random orientation of the crystallites.

One would like to use data such as those of Fig. 5, which shows the echoes for pure Be and the most dilute of our *Be*Ni samples, to determine $f(\omega_q)$. Unfortunately, for $I=\frac{3}{2}$ nuclei such as ^{9}Be, a dipole echo is superimposed on the quadrupole echo.[51] For the data of Fig. 5 the dipole and quadrupole echo decay times are comparable and it is not possible to separate the two effects.

The quadrupole echo in *Be*Ni narrows with increasing c_{Ni} —i.e., $f(\omega_q)$ broadens—as shown in Fig. 6. The half width of the echo for the $c_{\text{Ni}}=0.0355$ sample, $\tau=9$ μsec, corresponds to an "average" quadrupole splitting of $\Delta H=1/\gamma_n\tau=30$ Oe. Thus alloying Ni in Be produces a distribution of quadrupole splittings whose width is approximately the same as the splitting in pure Be.

The free-induction decays in *Be*Ni (Fig. 1) lengthen slightly with increasing c_{Ni}. The time for

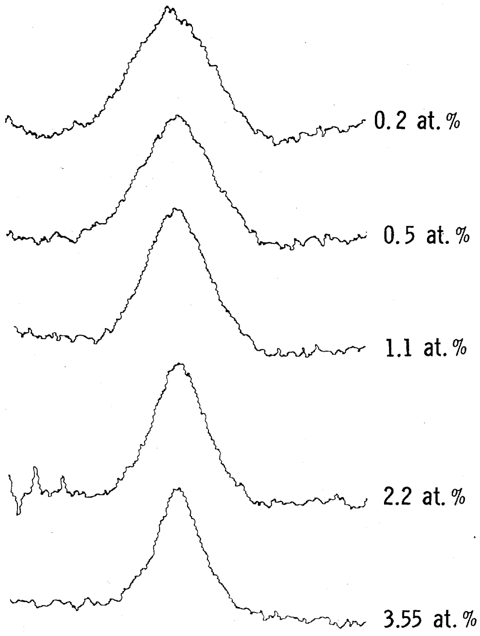

FIG. 6. ^{9}Be quadrupolar echoes in *Be*Ni samples at 295 K and 11.500 MHz. Ni concentrations are given in at.%. Only the center of the echo for the 0.2-at.% Ni sample is shown in this figure (cf. Fig. 5). 128 μsec full scale.

the decay to fall to half its initial amplitude is $\tau_{1/2} = 120$ μsec for the $c_{\rm Ni} = 0.002$ sample and $\tau_{1/2} = 170$ μsec for the $c_{\rm Ni} = 0.0355$ sample. It is well known that a large quadrupolar splitting causes a narrowing of the dipolar line (lengthening of the free-induction decay),[52] and the effect has been observed experimentally in alloys of copper.[31] The situation in *Be*Ni is somewhat more complicated than that of Cu alloys because ω_q exceeds the dipole interaction in pure Be, whereas $\omega_q = 0$ in pure well annealed Cu. However, many crystallites in a powder sample are so oriented that $\omega_q(3\cos^2\theta - 1)$ is small, and nuclei in such crystals experience quadrupole splittings which are smaller than the dipole linewidth. If ω_q increases while θ remains fixed, the fraction of crystallites having quadrupole splittings smaller than the dipole width decreases; thus the fraction of nuclei with narrowed lines increases, and a narrower overall line should result. We believe this explains the small increase of $\tau_{1/2}$ in Fig. 1.

IV. ANALYSES

A. Density of states at Fermi energy in Be: Electron-phonon mass enhancement parameter

At low temperatures Eq. (2) takes the form

$$(T_1T)^{-1} = (16\pi^3/9)k\hbar^3\gamma_e^2\gamma_n^2\langle |u(0)|^2\rangle^2_{E_F^0}[N(E_F^0)]^2 \ . \tag{11}$$

If the direct contact mechanism used to derive Eq. (11) is the dominant source of relaxation, as is usual in metals, and if the wave-function density at the nucleus, $A \equiv \langle |u(0)|^2\rangle_{E_F^0}$, is known, $N(E_F^0)$ can be calculated from the experimental T_1T.

We use $T_1T = (1.86 \pm 0.06) \times 10^4$ sec K, the average of the T_1T term we obtained in Sec. III B and the result Alloul and Froidevaux obtained at low temperatures.[24] Other determinations are excluded because they were made at higher temperatures where T_1T is not constant.

Values for A have been calculated by Gerstner and Cutler[23] (GC) and by Jena, Das, and Mahanti[53] (JDM). JDM have also calculated core-polarization terms, and their s-state core polarization can be added to the values of A to give a direct-plus-s-state core-polarization factor A^*, which we use instead of A (GC used the JDM core polarization when they calculated the Knight shift in Be). JDM attribute 68% of $1/T_1T$ to the direct contact mechanism, a number which increases to 96% when the s-state core polarization is added; the remaining 4% of their calculated $1/T_1T$ comes from p-state core polarization.[53, 54]

From the Knight-shift calculations of GC and JDM we readily obtain $A^*_{\rm GC} = 8.83$ and $A^*_{\rm JDM} = 6.71$ (the corresponding values for the conduction-electron wave-function density at the nucleus, averaged over the Fermi surface, are $A_{\rm GC} = 7.76$ and $A_{\rm JDM} = 5.64$).[55]

We thus obtain from Eq. (11)

$$N(E_F^0) = \begin{cases} 0.740 \pm 0.019({\rm GC}) \ , \\ 0.976 \pm 0.025({\rm JDM}) \ , \end{cases} \tag{12}$$

in states/Ry atom. The uncertainties in these results are propagated from the experimental uncertainty in T_1T; clearly the discrepancy between the GC and JDM values for A^* is more important than the propagated experimental uncertainties. In Table III the results of Eq. (12) are compared to values of $N(E_F^0)$ determined in calculations of the band structure of Be. The GC result lies slightly below, and the JDM result lies comfortably within, the rather wide band of theoretical predictions.

Wilk, Fehlner, and Vosko[13] (WFV) attribute the large spread in first-principles theoretical calculations of $N(E_F^0)$ to the methods used in calculating the density of states, rather than to the potentials used, or to inaccuracies in energy eigenfunctions. They point to the greater than 30% change in $N(E_F^0)$ that resulted when Loucks refined the calculation he and Cutler made[2] by carrying out the calculation at more points in the Brillouin zone. From this point of view the most reliable first-principles calculations of $N(E_F^0)$ should be those of Loucks[3] and of WFV[13]; the $N(E_F^0)$ of Tripp *et al.*,[6] which results from applying the pseudopotential method to fit de Haas-van Alphen frequencies, should also be considered.

The WFV comment about theoretical estimates of $N(E_F^0)$ applies with equal force to the values of A^* we used to obtain Eq. (12). The wave-function densities GC and JDM derived were both based on the potential of Loucks and Cutler.[2] The fact that such different results were obtained from the same potential demonstrates that considerable care is required in such calculations. A more definitive calculation of the magnetic hyperfine couplings in beryllium metal is the key to realizing the promise NMR holds for determining an accurate experimental value for $N(E_F^0)$.

Table III contains, in addition to theoretical densities of states, the values $N'(E_F)$ obtained from specific-heat experiments. The prime on the specific-heat density of states denotes the fact that it is enhanced by the electron-phonon interaction, whereas the NMR result is a "bare" density of states. The relation between the two is customarily expressed in the form

$$N'(E_F) = (1+\lambda)N(E_F) \ , \tag{13}$$

where λ is the electron-phonon mass enhancement parameter.[56]

Combining Eqs. (12) and (13) with the specific-

TABLE III. Densities of states at E_F for beryllium metal, from experiment and theory.

Source		Density of states at E_F, in states/Ry atom
This work	Using contact hyperfine interaction calculated by GC (Ref. 23)	0.740
	Using contact hyperfine interaction calculated by JDM (Ref. 53)	0.976
Specific heat	Ahlers (Ref. 16)	0.9882
	Gmelin (Ref. 15)	1.06
Theory	Herring and Hill (Ref. 1)	1.26
	Loucks and Cutler (Ref. 2)	1.31
	Loucks (Ref. 3)	0.957[a]
	Altmann and Bradley (Ref. 4)	1.35
	Terrell (Ref. 5)	0.8
	Tripp, Everett, Gordon, and Stark (Ref. 6)	0.85
	Taut (Ref. 8)	0.75[b]
	Inoue and Yamashita (Ref. 9)	0.962
	Nilsson, Arbman, and Gustaffson (Ref. 10)	1.07
	Bhokare and Yussouff (Ref. 11)	1.00
	Chatterjee and Sinha (Ref. 12)	1.48
	Wilk, Fehlner, and Vosko (Ref. 13)	0.907

[a] Calculated by Ahlers (Ref. 16) from Louck's work.

[b] Reference 8 treats three cases. The result given here is from the most complete of the calculations, denoted case 3 in Ref. 8.

heat results of Ahlers[16] (which is preferred because his sample was the purest of all those used in specific-heat studies), we find $\lambda = 0.25$ (GC) and 0.01 (JDM).

Grimvall recently reviewed electron-phonon interactions in metals, and concluded that $\lambda = 0.24 \pm 0.05$ for Be.[56] WFV argue that λ is not so accurately known, and give the range 0.16–0.29.[13] From our analysis of the NMR data we can conclude only that $\lambda \lesssim 0.25$. This again points up the need for a definitive calculation of the magnetic hyperfine interactions in Be metal.

The discussion above has omitted exchange-correlation enhancement effects and orbital contributions. WFV found the enhancement of the static spin susceptibility to be $\approx 8\%$ in Be. This 8% is an upper limit on the enhancement of $1/T_1$ because exchange enhancement of the static susceptibility is larger than enhancement of $1/T_1$.[57] Since $N(E_F^0) \propto (1/T_1)^{1/2}$, then, exchange enhancement should affect our results for $N(E_F^0)$ by less than 4%. This justifies our neglect of exchange enhancement.

The orbital contribution to $1/T_1$ has been calculated in the nearly free-electron approximation by Haga and Maeda.[58] We substitute in their Eq. (2.11) the values 0.0109 for $\langle (m^*/m)^2 \rangle$, the squared effective mass ratio averaged over the Fermi surface, determined by working backward from the GC diamagnetic Knight shift;[23] $E_F = 0.85$ Ry, a value typical of the band theory results; and

$$k_F = (2m^* E_F/\hbar^2)^{1/2} = 5.63 \times 10^7 \text{ cm}^{-1} \ .$$

The result is an orbital T_1 of ≈ 1200 sec at 300 K, as compared to an experimental value of 58 sec. Thus orbital effects on $1/T_1$ can be neglected, as they are comparable to the uncertainty in the experimental value.

Finally, we note that we can use Eqs. (8) and (12) to determine the value of $[\partial^2 N(E)/\partial E^2]_{E_F^0}$. The results, in units of states/Ry^3 atom, are 7.4×10^3 (GC) and 9.7×10^3 (JDM).

B. Effect of alloying with Ni on the electronic structure of Be

Taking the differential of Eq. (11), we find

$$\delta(1/T_1T) = \tfrac{8}{3}\pi^{3/2}\hbar^{3/2}k^{1/2}\gamma_e\gamma_n(T_1T)^{-1/2} \times [\delta(A^*)N(E_F^0) + A^*\delta(N(E_F^0))] \ , \quad (14)$$

where $\delta(\cdots)$ denotes the change in the quantity in parentheses with alloying, and where A^* has been used instead of A. Equation (14) is used to obtain $\delta(A^*)$, the "average" change in A^* due to alloying Ni in Be.

To obtain $\delta(1/T_1T)$ we use the average of the room temperature T_1s for $c_{\mathrm{Ni}}=0.002$, 0.005, and 0.011 samples (Table II), statistically weighted according to their respective experimental uncertainties and normalized to $c_{\mathrm{Ni}}=0.010$. As pointed out in Sec. III B, room-temperature relaxation rates are slightly enhanced relative to the $(T_1T)^{-1}$ assumed in Eq. (14). Therefore the correction factor (1.72/1.86), the ratio of the experimental room temperature pure Be T_1T to the correct linear term, is applied to the room temperature T_1T for each *Be*Ni alloy.

The $N(E_F^0)$ values we use in Eq. (14) are taken from Eq. (12). The $\delta(N(E_F^0))$ values, 0.155 and 0.125 states/Ry at.% Ni, are derived from the Klein-Heeger specific-heat density of states in *Be*Ni, 0.0846 states/Ry Ni atom,[27] by dividing by the factors $(1+\lambda)$ appropriate to the GC and JDM cases, respectively. The values of A^* are taken from the previous section of this paper.

Putting these values of parameters into Eq. (14) we obtain (in cm^{-3})

$$\delta(A^*)=\begin{cases}0.80(\mathrm{GC}) \; ,\\ 0.88(\mathrm{JDM}) \; .\end{cases} \tag{15}$$

The GC result is a 9% change in the electron charge density at the Be nucleus, and the JDM result is a 13% change. These $\delta(A^*)$'s represent a kind of average over Be sites of the damped oscillatory charge distribution which presumably surrounds the solutes.[29] Substituting Eq. (12), Eq. (15), and the specific-heat data into Eq. (14), we find that approximately 60% of the additional host spin-lattice relaxation due to alloying Ni in Be can be ascribed to enhancement of the electron density of states at the Fermi surface, $\delta(N(E_F^0))$, and approximately 40% to $\delta(A^*)$.

To analyze the change in Knight shift $\delta(\mathcal{K})$ with dilute alloying, we assume $\delta(\mathcal{K})$ can be written in a manner similar to Eq. (14)

$$\delta(\mathcal{K})=(\tfrac{8}{3}\pi)[A^*\delta(\chi_s)+\delta(A^*)\chi_s] \; , \tag{16}$$

where χ_s is the paramagnetic susceptibility of the mobile electrons. The average of the three experimental determinations of χ_s in pure Be is 1.8×10^{-7} cgs volume units.[17–19] If we assume the increase in bulk susceptibility with alloying is pure electron-spin susceptibility, as Klein and Heeger did in analyzing their *Be*Ni data,[27] $\delta(\chi_s)=\delta(\chi_{\mathrm{total}})=4.4\times10^{-7}$ cgs volume unit per at.% Ni, where $\delta(\chi_{\mathrm{total}})$ is obtained from Fig. 3 of Ref. 27.[59]

Then, using the theoretical values for A^*, and assuming the values of $\delta(A^*)$ in Eq. (15) may be used in Eq. (16), we find, in ppm/at.% Ni

$$\delta(\mathcal{K})=\begin{cases}33.8(\mathrm{GC}) \; ,\\ 26.0(\mathrm{JDM}) \; .\end{cases} \tag{17}$$

These numerical results are almost entirely due to the first term of Eq. (16), because $A^* \gg \delta(A^*)$ and $\chi_s \approx \delta(\chi_s)$. The results are displayed as the straight lines in Fig. 4, which have been made to pass through the experimental point for $c_{\mathrm{Ni}}=0.011$. In view of the scatter in Knight shifts measured for pure Be, one cannot say definitively whether the GC or JDM result is to be preferred. Both give rather good agreement with experiment (Fig. 4), lending a measure of internal consistency to our elementary analysis of the alloy T_1 and Knight-shift data—an analysis which has relied on a number of plausible but unproven assumptions.

Our results and those of Klein and Heeger show Ni induces significant quantitiative changes in the electronic structure of Be. One atomic percent of Ni in Be produces approximately a 15% increase in the density of states at the Fermi surface, 240% increase in the spin susceptibility, and 10% increase in the "average" electron density at the Be sites.

C. The electron-spin susceptibility of pure Be

For a long time the electron-spin susceptibility of beryllium has puzzled observers. The spin susceptibility determined by conduction-electron-spin-resonance (CESR) experiments, $\chi_s=1.8\times10^{-7}$ cgs volume units,[17–19] is less than half the Pauli susceptibility, $\chi_P=\frac{1}{4}\gamma_e^2\hbar^2N(E_F^0)$, calculated from the theoretical band-structure density of states or from the experimental specific-heat density of states. Such a large discrepancy is difficult to rationalize.

WFV recently attacked this problem,[13] using theoretical techniques that had accounted successfully for χ_s in alkali metals.[60] WFV used a variational method to evaluate exchange-correlation functionals which appear in spin-density functional theory, and thereby obtained a theoretical lower bound for χ_s. The single-particle density of states appears in this theory, and it was determined from augmented plane wave (APW) muffin-tin calculations at 640 points in the irreducible segment of the Brillouin zone. The theoretical result, $\chi_s \gtrsim 4.7\times10^{-7}$ cgs volume units, is still more than a factor of 2 larger than the CESR susceptibility. This led WFV to question the CESR result.

We agree that the experimental situation is unclear. The published CESR susceptibilities were obtained by applying Dyson's theory[61] to the experimental data, but Dyson's theory does not work well for beryllium.[19] Extension of Dyson's theory to noncubic systems which are not purely free electron like would therefore be more useful than new CESR data.

In principle, our NMR data for *Be*Ni could be combined with Eq. (16) to obtain a new experimental value for χ_s. However, as we mentioned in connection with Eq. (17), the $\delta(A^*)\chi_s$ term in Eq. (16) accounts for only a few percent of the total change in the Knight shift due to alloying. An alloy for which $\delta(\chi_s) \approx 0$ would be required for this line of analysis. Moreover, A^* is not known with sufficient accuracy. More definite observations should be possible on the basis of the pure-metal T_1 and Knight shift.

$N(E_F^0)$s determined from T_1 data agree well with the results of band theory (Table III). Even the rather low $N(E_F^0)$ obtained with the GC value of A^* yields a Pauli susceptibility, $\chi_P = 3.6 \times 10^{-7}$ cgs volume units, which is two times the CESR value [χ_P is a reasonable numerical approximation to the WFV susceptibility in Be; for example, χ_P calculated with the $N(E_F^0)$ from WFV differs from the WFV χ_s by only about 6%]. Unless something is drastically wrong with our understanding of the relation between χ_s and $N(E_F^0)$, the T_1 results support the contention that theoretical values of χ_s are more reliable than the CESR value.

On the other hand, the Knight shift data do not obviously support such a contention. The two theoretical values, $\mathcal{K} = -41$ ppm (calculated by GC) and $\mathcal{K} = -44$ ppm (obtained by adding the GC diamagnetic shift to the JDM contact-plus core-polarization shift), are more negative than the average of the experimental values, $\mathcal{K} = -21$ ppm. If χ_s were assumed to be approximately two times the CESR value, as WFV assert, the theoretical Knight shifts would become $\mathcal{K} \approx -85$ ppm because, in the GC theory for the Knight shift,[23] all contributions to $\mathcal{K}$ are proportional to χ_s. Therefore, the discrepancy between theoretical and experimental values for $\mathcal{K}$ is increased by discarding the CESR value of χ_s.

T_1 and $\mathcal{K}$ thus appear to lead to inconsistent conclusions about the value of χ_s, T_1 saying the CESR value is at least a factor of 2 too small, and $\mathcal{K}$ saying the CESR value is approximately correct. Evidently, the theoretical bases for interpreting T_1 and $\mathcal{K}$ in Be need further scrutiny.

We believe the interpretation of T_1 presented in Sec. IV A is correct in its essentials. No sources of spin-lattice relaxation have been omitted from consideration which, at the temperatures considered here, should be significant when compared to the contact-plus core-polarization contribution. However, one cannot, in our opinion, be confident about the accuracy of the theoretical Knight shift. Because the sum of the direct contact and core-polarization contributions to $\mathcal{K}$ is nearly zero, the accuracy of the theoretical value of $\mathcal{K}$ is governed by the accuracy of the theoretical value of the diamagnetic contribution, $\mathcal{K}_{\text{dia}}$.

GC calculated $\mathcal{K}_{\text{dia}}$ from

$$\mathcal{K}_{\text{dia}} = (\tfrac{8}{3}\pi)\chi_{\text{dia}} \;, \tag{18a}$$

$$= -(\tfrac{8}{9}\pi)\langle (m/m^*)^2 \rangle \chi_s \;, \tag{18b}$$

where the angle brackets denote an average over the Fermi surface of $(m/m^*)^2$, the square of the ratio of the mass of the free electron to the effective mass of the electron. The Landau-Peierls diamagnetism[62] is used for χ_{dia} to obtain Eq. (18b).

Unfortunately for such an analysis, the Landau-Peierls diamagnetism is not the only contribution that could be significant. On some portions of the Fermi surface of Be, $m^*/m \approx 0.02$.[6] Thus, there are bands close in energy to the conduction bands, which interact with them, and which cause contributions to χ_{dia} that can have the same order of magnitude as the Landau-Peierls susceptibility.[62]

Stephen and Hebborn have derived formulas for the diamagnetic shielding of nuclei by Bloch electrons in metals and conclude that in general one should expect significant corrections to the Landau-Peierls contributions to $\mathcal{K}_{\text{dia}}$.[63] The complete formula for $\mathcal{K}_{\text{dia}}$ contains second derivatives of Bloch wave functions and third derivatives of energy values, however, and so numerical evaluation would be a formidable task.

Instead of proceeding via Eq. (18b), we might calculate

$$\chi_{\text{dia}} = \chi_{\text{total}} - \chi_s - \chi_{\text{ion core}} \tag{19}$$

and combine it with Eq. (18a) to obtain $\mathcal{K}_{\text{dia}}$.[64] Use of $\chi_{\text{total}} = -24.32 \times 10^{-7}$,[18] $\chi_{\text{ion core}} = 0.76 \times 10^{-7}$,[65] and $\chi_s = 1.8 \times 10^{-7}$ cgs volume units (the average CESR value[17-19]) yields $\mathcal{K}_{\text{dia}} = -21$ ppm.

Combining this with the direct contact and core-polarization contributions results in the total calculated Knight shift (in ppm),

$$\mathcal{K} = \begin{cases} -11(\text{GC}) \\ -14(\text{JDM}) \end{cases} \tag{20}$$

in Be metal.

The Knight shifts obtained via Eq. (18b), on the one hand, and Eq. (19) on the other, bracket the average value of the experimental Knight shift, -21 ppm, with Eq. (19) giving somewhat better agreement. This demonstrates the dominance of the diamagnetic shift in Be metal. A more rigorous numerical calculation of the diamagnetic term for Be would be of great interest.

If the WFV value, $\chi_s = 4.7 \times 10^{-7}$ cgs volume units, is used in Eq. (19) instead of the CESR value, $\mathcal{K}_{\text{dia}} = -23$ ppm results. The calculated contact and core-polarization shifts are also affected by this change in χ_s; the new values of the total Knight shifts, corresponding to Eq. (20), are $\mathcal{K} = -1$ ppm (GC) and -6 ppm (JDM).

The CESR value of χ_s, therefore, produces better agreement with the experimental Knight shift than the band theory value does, whether one approaches the calculation via Eq. (18b) or via Eqs. (19) and (18a). It is interesting, however, that in one case the WFV susceptibility overestimates the magnitude of the (negative) Knight shift, but in the other case underestimates it. This is probably due to the approximate nature of the expressions we have used for the diamagnetic contribution, and does not conclusively demonstrate the superiority of the CESR susceptibility in interpreting the Knight shift.

V. SUMMARY

We have measured the ^{9}Be shift, $\mathcal{K}$, in *Be*Ni alloys, and the nuclear spin-lattice relaxation time, T_1, in pure Be and *Be*Ni.

$T_1 T$ is constant in Be and *Be*Ni below room temperature. For $T \gtrsim 300$ K, $1/T_1 T$ is enhanced above the low-temperature value, but the ratio of $(T_1)_{\rm Be}$ to $(T_1)_{Be\rm Ni}$ remains constant throughout the entire temperature range, 77–525 K, over which we conducted measurements. We have quantitatively accounted for this anomalous temperature dependence of the Be and *Be*Ni T_1 in terms of the thermal broadening of the Fermi distribution in the presence of the deep valley in the Be electron density of states near the Fermi energy.

From our analysis of T_1 vs T we obtain for the term linear in T, $T_1 T = (1.87 \pm 0.05) \times 10^4$ sec K for pure Be; averaging this with the low-temperature result of Alloul and Froidevaux results in $T_1 T = (1.86 \pm 0.06) \times 10^4$ sec K.

We have used the T_1 results, together with theoretical hyperfine interactions, to calculate the electron density of states, $N(E_F^0)$, at the Fermi energy in Be, and the electron-phonon mass enhancement parameter, λ. The two theoretical results for the contact hyperfine interaction yield $N(E_F^0) = 0.74$ states/Ry atom and $\lambda = 0.25$ (GC), and $N(E_F^0) = 0.98$ states/Ry atom and $\lambda = 0.01$ (JDM).

$1/T_1$ in *Be*Ni is proportional to $c_{\rm Ni}$ for $c_{\rm Ni} \lesssim 0.01$. Using a model based on the contact hyperfine interaction, we find that approximately 60% of this increase can be ascribed to an increase in $N(E_F^0)$ with alloying, and approximately 40% to an increase in the hyperfine coupling averaged (in an NMR sense) over Be atoms. When these results are used, together with the CESR spin susceptibility and the increase in bulk susceptibility measured by Klein and Heeger, the initial slope of Knight shift versus $c_{\rm Ni}$ is successfully predicted.

We examine the anomalous electron-spin susceptibility of Be in the light of NMR data. $N(E_F^0)$ from T_1 data support the contention of Wilk, Fehlner, and Vosko that the susceptibility determined from CESR data is too small. On the other hand, agreement between theoretical Knight-shift calculations and experimental data for $\mathcal{K}$ is better if one uses the smaller CESR susceptibilities. However, the latter calculations are too approximate to permit firm conclusions to be drawn.

ACKNOWLEDGMENT

The assistance of Mr. Kenneth Blacker in performing these experiments is greatly appreciated.

---

*Now at GTE Laboratories, Inc., Waltham, Mass. 02154.

[1] C. Herring and A. G. Hill, Phys. Rev. 58, 132 (1940).

[2] T. L. Loucks, and P. H. Cutler, Phys. Rev. 133, A819 (1964).

[3] T. L. Loucks, Phys. Rev. 134, A1618 (1964).

[4] S. L. Altmann and C. J. Bradley, Proc. Phys. Soc. London 86, 915 (1964).

[5] J. H. Terrell, Phys. Rev. 149, 526 (1966).

[6] J. H. Tripp, P. M. Everett, W. L. Gordon, and R. W. Stark, Phys. Rev. 180, 669 (1969).

[7] J. H. Tripp, Phys. Rev. B 1, 550 (1970).

[8] M. Taut, Phys. Status Solidi B 54, 149 (1972).

[9] S. T. Inoue and J. Yamashita, J. Phys. Soc. Jpn. 35, 677 (1973).

[10] P. O. Nilsson, G. Arbman, and T. Gustafsson, J. Phys. F 4, 1937 (1974).

[11] V. V. Bhokare and M. Yussouff, Nuovo Cimento B 19, 149 (1974).

[12] S. Chatterjee and P. Sinha, J. Phys. F 5, 2089 (1975).

[13] L. Wilk, W. R. Fehlner, and S. H. Vosko, Can. J. Phys. 56, 266 (1978). In the text this work is denoted WFV.

[14] See, especially, the discussion of Fig. 7 in Ref. 13.

[15] M. E. Gmelin, C. R. Acad. Sci. 249, 3459 (1964).

[16] G. Ahlers, Phys. Rev. 145, 419 (1966).

[17] G. Feher and A. F. Kip, Phys. Rev. 98, 337 (1955).

[18] C. S. Bowring and V. T. Wynn, Phys. Lett. A 33, 401 (1970).

[19] J. H. Orchard-Webb, A. J. Watts, M. A. Smithard, and J. E. Cousins, Phys. Status Solidi 41, 325 (1970).

[20] D. E. Barnaal, R. G. Barnes, B. R. McCart, L. W. Mohn, and D. R. Torgeson, Phys. Rev. 157, 510 (1967).

[21] W. T. Anderson, Jr., M. Ruhlig, and R. R. Hewitt, Phys. Rev. 161, 293 (1967).

[22] M. Mehring and H. Raber, Solid State Commun. 13, 1637 (1973).

[23] J. Gerstner and P. H. Cutler, Phys. Lett. A 30, 368 (1969). A revision of the diamagnetic contribution to the Knight shift is given in J. Gerstner and P. H. Cutler, Nat. Bur. Stand. (U.S.) Spec. Publ. 323, 649 (1971). In the text this work is denoted GC.

[24] H. Alloul and C. Froidevaux, J. Phys. Chem. Solids 29, 1623 (1968).

[25] P. L. Sagalyn, J. A. Hofmann, and M. E. Schillachi, Bull. Am. Phys. Soc. 11, 916 (1966).

[26] Y. Chabre, J. Phys. F 4, 626 (1974).

[27] A. P. Klein and A. J. Heeger, Phys. Rev. 144, 458 (1966).

[28] P. W. Anderson, Phys. Rev. 124, 41 (1961).

[29] J. Friedel, Can. J. Phys. 34, 1190 (1956); *Metallic Solid Solutions* (Benjamin, New York, 1963), Chap. XIX.

[30] A. Narath, J. Appl. Phys. 41, 1122 (1970); Crit. Rev. Solid State Sci. 3, 1 (1972).

[31] A. T. Fromhold, Jr., J. Chem. Phys. 52, 2871 (1970).

[32] J. B. Hess, Acta Crystallogr. 4, 209 (1951).

[33] J. B. Nelson and D. P. Riley, Proc. Phys. Soc. London 57, 160 (1945).

[34] A. A. Cox and E. G. Steward, Acta Crystallogr. 23, 1113 (1967).

[35] M. N. Alexander, Phys. Rev. 172, 331 (1968).

[36] I. J. Lowe and R. E. Norberg, Phys. Rev. 107, 46 (1957).

[37] The (on-resonance) free induction decay of a pair of spins interacting via the dipolar interaction and experiencing a quadrupolar splitting larger than the dipolar broadening but smaller than H_1 may be shown to have the form

$$S(t)\propto e^{i\gamma H_0 t/\hbar}\sum_{m=-3/2}^{+3/2}\left[\langle m-\tfrac{1}{2}|\mathcal{O}|m\ \tfrac{1}{2}\rangle+\sqrt{3}\langle m\ \tfrac{1}{2}|\mathcal{O}|m\ \tfrac{3}{2}\rangle\cos\alpha t\right]\;,$$

where γ is the nuclear gyromagnetic ratio, H_0 is the external magnetic field, $\mathcal{O}=e^{-iH_D t/\hbar}I_x e^{iH_D t/\hbar}$ (a 90° pulse is assumed), H_D is the truncated dipolar Hamiltonian, α measures the strength of the quadrupole interaction, and m is the magnetic quantum number for a single spin; we have assumed the nuclear spin $I=\frac{3}{2}$ appropriate to beryllium.

[38] C. Rizzuto, Rep. Prog. Phys. 37, 147 (1974).

[39] C. P. Slichter, *Principles of Magnetic Resonance*, 2nd ed. (Springer-Verlag, Berlin, 1978), pp. 144–148.

[40] J. M. Ziman, *Principles of the Theory of Solids* (Cambridge University Press, Cambridge, 1964), p. 119, Eqs. (4.21) and (4.23).

[41] P. Jena and T. P. Das, Phys. Rev. B 4, 3931 (1971).

[42] J. M. Winter, *Magnetic Resonance in Metals* (Oxford University Press, London, 1971), p. 116.

[43] M. Yamaguchi, Y. Takahashi, Y. Takasaki, and T. Ohta, Bull. Fac. Eng. Yokohama Nat. Univ. 23, 175 (1974).

[44] M. Mehring, *High Resolution NMR Spectroscopy in Solids* (Springer-Verlag, Berlin, 1976), pp. 62–63.

[45] Walter Clark Hamilton, *Statistics in Physical Science* (Ronald, New York, 1964), Sec. 2–7.

[46] W. T. Anderson, Jr., F. C. Thatcher, and R. R. Hewitt, Phys. Rev. 171, 541 (1968).

[47] An earlier measurement of the Knight shift for the $c_{\mathrm{Ni}}=0.022$ sample [J. A. Hofmann, P. L. Sagalyn, and J. Greespan, Bull. Am. Phys. Soc. 12, 314 (1966)] yielded −40 ppm, whereas the present pulse measurement yields +8 ppm. The older determination was made with a cw marginal oscillator, which operates in pure absorption mode. We examined our powder samples under the microscope. The particles in the $c_{\mathrm{Ni}}=0.022$ powders were smooth, and had diameters of $3-8\times10^{-3}$ cm, considerably greater than the diameters of particles for the other samples. The rf skin depth in the cw measurements on the $c_{\mathrm{Ni}}=0.022$ sample would have been typically 9.5×10^{-3} cm. In most experiments this ratio of particle size to skin depth would be acceptable, especially since comminuted powders usually contain jagged particles (which decreases the effective ratio of particle size to rf skin depth). We find, applying the methods A. C. Chapman, P. Rhodes, and E. F. W. Seymour [Proc. Phys. Soc. London 70, 345 (1957)] used for NMR in "thick" metal plates, that the center of the $c_{\mathrm{Ni}}=0.022$ lock-in absorption mode line would be shifted 26–53 ppm in the direction corresponding to a negative Knight shift. This is approximately the difference between the older measurement and the current one. Moreover, the analysis of Chapman, Rhodes, and Seymour predicts a small asymmetry in the lock-in line which is present in the older data. We note, incidentally, that sample particle sizes are not given in Refs. 20–22, which report experimental Knight shifts in Be metal.

[48] M. Mehring (private communication); M. Mehring, D. Kotzur, and O. Kanert, Phys. Status Solidi B 53, K25 (1972).

[49] I. Solomon, Phys. Rev. 110, 61 (1958); G. Bonera and M. Galimberti, Solid State Commun. 4, 589 (1966); I. D. Weisman and L. H. Bennett, Phys. Rev. 181, 1341 (1969).

[50] Reference 39, Chap. 9.

[51] W. W. Warren, Jr., and R. E. Norberg, Phys. Rev. 154, 277 (1967).

[52] K. Kambe and J. F. Ollom, J. Phys. Soc. Jpn. 11, 50 (1956); A. Abragam, *Principles of Nuclear Magnetism* (Oxford University Press, London, 1961), p. 128ff.

[53] P. Jena, T. P. Das, and S. D. Mahanti, Phys. Rev. B 1, 432 (1970). In the text this work is denoted JDM.

[54] Reference 53 considerably overestimates the value of $1/T_1T$. This appears to be due to use of the rather large estimate of $N(E_F^0)$ in Ref. 2 (see Table III). When the smaller values of $N(E_F^0)$ based on finer-grained division of the Brillouin zone (Refs. 3 and 13) are used, $1/T_1T$ is underestimated.

[55] Following Slichter (Ref. 39) we write

$$\mathcal{K}=(8\pi/3)\chi_s\langle|u(0)|^2\rangle_{E_F}=(8\pi/3)\chi_s A$$

for the direct contact Knight shift, and analogously for A^* when core polarization is included. Thus the normalization volume, made the unit of volume, is the atomic volume. In Ref. 23 (GC) and in Ref. 53 (JDM) the wave function is normalized in an atomic cell.

[56] G. Grimvall, Phys. Scr. 14, 63 (1976).

[57] A. Narath, H. T. Weaver, Phys. Rev. 175, 373 (1968).

[58] E. Haga and S. Maeda, J. Phys. Soc. Jpn. 33, 1258 (1972).

[59] It is difficult to make direct links between solute and host NMR studies, particularly when the solute is a transition metal. Nevertheless it is interesting that Narath found the fraction of the *Be*Ni impurity Knight shift attributable to orbital paramagnetism to be anomalously small (Ref. 30). This is consistent with our assumption that the increase in susceptibility associated with Ni in Be can be ascribed to spin, rather than orbital, susceptibility.

[60] A. H. MacDonald and S. H. Vosko, J. Low Temp. Phys. 25, 27 (1976).

[61] F. J. Dyson, Phys. Rev. 98, 349 (1955).

[62] H. J. Zeiger and G. W. Pratt, *Magnetic Interactions in Solids* (Oxford University Press, London, 1973), Sec. 5.6.

[63] M. J. Stephen, Proc. Phys. Soc. London 79, 987 (1962); M. J. Stephen and J. E. Hebborn, *ibid.* 80, 991 (1962); J. E. Hebborn, *ibid.* 80, 1237 (1962).

[64] This was done earlier by E. Borchi and S. De Gennaro, Lett. Nuovo Cimento 6, 111 (1973). We use somewhat different numerical inputs and make a different discussion.

[65] Charlotte Froese Fischer (unpublished). We thank Dr. R. J. Weiss for making this result available to us.